THE JOURNAL OF BIOLOGICAL CHEMISTRY VOL. 287, NO. 28, pp. 23971–23976, July 6, 2012

Structural Basis for Activation of an Integral Membrane Protease by Lipopolysaccharide

Received for publication, April 26, 2012, and in revised form, May 23, 2012 Published, JBC Papers in Press, May 29, 2012, DOI 10.1074/jbc.M112.376418

Elif Eren and Bert van den Berg[1]

From the Program in Molecular Medicine, University of Massachusetts Medical School, Worcester, Massachusetts 01605

Background: Lipids play an important role in membrane protein function (lipid allostery).
Results: The co-crystal structure of lipid-free Pla protease and a substrate peptide shows that the substrate displaces the active site nucleophilic water molecule.
Conclusion: Removal of LPS from Pla causes subtle conformational changes that inactivate the enzyme.
Significance: The structure provides the first explanation for lipid allostery of an outer membrane protein.

Omptins constitute a unique family of outer membrane proteases that are widespread in Enterobacteriaceae. The plasminogen activator (Pla) of *Yersinia pestis* is an omptin family member that is very important for development of both bubonic and pneumonic plague. The physiological function of Pla is to cleave (activate) human plasminogen to form the plasma protease plasmin. Uniquely, lipopolysaccharide (LPS) is essential for the catalytic activity of all omptins, including Pla. Why omptins require LPS for enzymatic activity is unknown. Here, we report the co-crystal structure of LPS-free Pla in complex with the activation loop peptide of human plasminogen, its natural substrate. The structure shows that in the absence of LPS, the peptide substrate binds deep within the active site groove and displaces the nucleophilic water molecule, providing an explanation for the dependence of omptins on LPS for enzymatic activity.

It is becoming increasingly clear that membrane lipids do not just provide a suitable but inert environment for membrane proteins, but that they can also directly modulate membrane protein function, a phenomenon dubbed "lipid allostery" (1). The biological function of membrane proteins can be affected by membrane lipid composition as well as by specific protein-lipid interactions. Examples of the latter class are the interaction of cholesterol with G protein-coupled receptors and the activation of the inward rectified K^+ channel Kir2.2 by phosphatidylinositol 4,5-bisphosphate (2, 3). To date, however, no explanation for the modulation of bacterial outer membrane (OM)[2] protein function by membrane lipids has been reported.

Yersinia pestis, a highly pathogenic bacterium, is the causative agent of plague in humans and has been classified by the Centers for Disease Control and Prevention as a Category A microbe. An important virulence factor of *Y. pestis* is the 292-amino acid long OM protease Pla (plasminogen activator), the physiological function of which is to activate (cleave) human plasminogen to generate the circulating serine protease plasmin. Plasmin degrades fibrin clots (fibrinolysis), noncollagenous proteins of base membranes and the extracellular matrix, to facilitate cell migration (4). Pla has been shown to be essential for development of bubonic plague by facilitating rapid dissemination of bacteria from the initial site of infection (5). Pla is also important for the progression of pneumonic plague, because it allows *Y. pestis* to replicate rapidly in lungs (6).

Pla belongs to a unique family of OM proteases known as omptins, which are widely distributed in Gram-negative bacterial pathogens that infect humans and plants (7–9). Omptins share high sequence identities (40–74%). The solved structures of two members of the family, *Escherichia coli* OmpT (10) and *Y. pestis* Pla (11), show that they have very similar structures with a barrel composed of 10 antiparallel transmembrane β-strands connected by five long extracellular loops. Despite their high identity and structural similarity, omptins differ greatly in their target specificity for proteolysis, invasive/adhesive properties, and virulence association, probably due to adaptations to the life style of the host bacterium (7–9).

Omptins appear to constitute a unique class of proteases because their conserved active site residues (Asp^{84}, Asp^{86}, Asp^{206}, and His^{208} in Pla, Fig. 1) differ from the active site consensus sequences found in serine, aspartic or metalloproteases. Crystal structures, mutagenesis studies, and molecular dynamics simulations for OmpT suggest a unique catalytic mechanism for proteases (10, 12, 13). According to this proposed mechanism, the catalytic Asp^{206}-His^{208} dyad activates a nucleophilic water molecule that attacks the scissile carbonyl carbon atom. The Asp^{84}-Asp^{86} dyad likely coordinates the nucleophilic water molecule either directly or indirectly via another water molecule (Fig. 1). In addition to the active site residues, both Ser^{99} and His^{101} located close to the active site have been shown to be important for omptin activity (14) because they coordinate the Asp^{84}-Asp^{86} dyad via bridging water molecules (12) (Fig. 1).

Another unique feature of omptins is that catalytic activity requires the presence of bound lipopolysaccharide (LPS), a complex glycolipid that makes up the outer leaflet of the OM.

The atomic coordinates and structure factors (code 4DCB) have been deposited in the Protein Data Bank, Research Collaboratory for Structural Bioinformatics, Rutgers University, New Brunswick, NJ (http://www.rcsb.org/).

[1] To whom correspondence should be addressed: Program in Molecular Medicine, University of Massachusetts Medical School, 373 Plantation St., Worcester, MA 01605. Tel.: 508-856-1201; Fax: 508-856-4289; E-mail: bert.vandenberg@umassmed.edu.

[2] The abbreviations used are: OM, outer membrane; Alp11, 11-residue activation loop peptide of human plasminogen; LDAO, *n*-dodecyl-*N*,*N*-dimethylamine-*N*-oxide; PDB, Protein Data Bank; Pla, plasminogen activator.

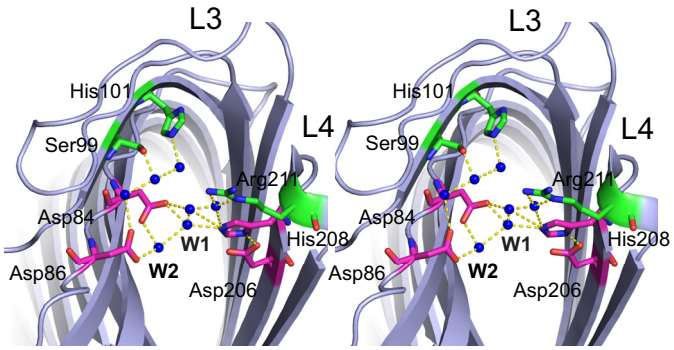

FIGURE 1. **Stereoview of the Pla active site viewed from the extracellular side (PDB ID 2X55).** The active site residues (Asn^{84}, Asp^{86}, Asp^{206}, and His^{208}) are shown in *magenta*; the other residues that are important for activity are shown in *green* (Ser^{99}, His^{101}, and Arg^{211}). Active site water molecules are shown as *blue spheres*. The nucleophilic water is labeled *W1*, and the water molecule between the Asp^{84}-Asp^{86} dyad is labeled *W2*. Hydrogen bonding of water molecules and amino acids are shown as *yellow dashes*.

LPS binds at a defined position on the outside of the barrel (14–16). Although crystal structures of apo-Pla in the absence and presence of bound LPS showed a subtle narrowing of the active site groove in the presence of LPS (13), it is unclear how this conformational change could activate the enzyme.

EXPERIMENTAL PROCEDURES

Purification of Pla for Crystallization—Cloning, expression, and site-directed mutagenesis of Pla (D84N) were carried out as described previously (11). BL21(DE3) T1 phage-resistant cells (New England Biolabs) were transformed with the pB22-Pla D84N construct. The cells were grown to $A_{600} \sim 0.6$ at 37 °C and then induced with 0.1% arabinose at 20 °C overnight. Cells were harvested by centrifugation at 4500 rpm for 30 min (J6-MC; Beckman Coulter). Cell pellets were suspended in TSB (20 mM Tris, 300 mM NaCl, 10% glycerol, pH 8.0), and cells were lysed by sonication (3 × 40-s intervals) (Branson Digital Sonifier). Total membranes were obtained by centrifugation at 40,000 rpm for 40 min (Ti-45 rotor, Beckman L8-70M ultracentrifuge). Membranes were homogenized in TSB and solubilized in 1% *n*-dodecyl-*N*,*N*-dimethylamine-*N*-oxide (LDAO; Anatrace) for 1 h at 4 °C followed by centrifugation at 40,000 rpm for 30 min to remove precipitates and unsolubilized membranes. The membrane extract was applied to a 10-ml nickel column. The column was washed with 10 column volumes of TSB containing 0.2% LDAO and 15 mM imidazole. The proteins were eluted with 3 column volumes of TSB containing 0.2% LDAO and 200 mM imidazole. The proteins were further purified by gel filtration chromatography using 10 mM Tris, 50 mM NaCl, and 0.05% LDAO, pH 8.0. For final polishing and detergent exchange, another gel filtration chromatography column was performed in 10 mM Tris, 100 mM LiCl, 0.35% C_8E_4, 0.05% decyl-β-maltoside, pH 8.0. The purified protein was concentrated to 10–15 mg/ml using 50-kDa molecular mass cutoff filters (Amicon), dialyzed overnight against gel filtration buffer, and flash-frozen in liquid nitrogen. For the preparation of active Pla used for cleavage of the activation loop peptide, protein was extracted in 1.5% β-octylglucoside to prevent loss of bound LPS (11). The nickel column and the first gel filtration column were also done in β-octylglucoside (0.8%).

TABLE 1
Data collection and refinement statistics

Parameters	Pla-Alp11
Data collection	
Space group	I222
Cell dimensions	
a, *b*, *c* (Å)	52.4, 63.1, 201.2
α, β, γ (°)	90.0, 90.0, 90.0
Resolution (Å)	50-2.03
R_{sym} or R_{merge}	10.1 (42.7)[a]
$I/\sigma I$	23.4 (5.2)
Completeness (%)	99.8 (99.7)
Redundancy	5.5 (5.1)
Refinement	
Resolution (Å)	19.8-2.03
No. reflections	20,964 (1,917)
R_{work}/R_{free}	18.04/23.19
No. atoms	
Protein	2,203
Peptide	64
Detergent/ion	21/5
Water	106
B-factors	
Protein	33.1
Peptide	57.4
Detergent/ion	46.8
Water	38.5
Root mean square deviations	
Bond lengths (Å)	0.008
Bond angles (°)	1.156

[a] Values in parentheses are for the highest resolution shell.

Crystallization of Pla-Alp11 and Structure Determination—An 11-residue activation loop peptide of human plasminogen (Alp11) with the sequence ^{557}KCPG**RV**VGGCK^{567} was synthesized (Biomatik, Wilmington, DE) with the substitution V567K (numbering for intact human plasminogen) to increase solubility. The peptide was dissolved in protein buffer and added to Pla D84N at a final concentration of ~10 mM. Hanging-drop crystallization trials were set up using several commercial screens (MemGold and Structure I/II). Several initial hits were obtained, and one of those (Structure II/#8) was optimized to give thin plates that grew to sufficient size after several weeks of incubation. The crystals were obtained by adding 1 μl of protein-peptide solution to 1 μl of mother liquor containing 45% (v/v) 2-methyl-2,4-pentanediol, 0.2 M $NH_4KH_2PO_4$, and 0.1 M NaOAc, pH 5.5. The crystals of the complex belonged to space group I222 and contained one molecule/asymmetric unit. Crystals were flash-frozen in liquid nitrogen directly from the mother liquor.

Diffraction data were collected at 100 K at the National Synchrotron Light Source (Brookhaven National Laboratory) at beamline X6A and processed with HKL2000 (17). The crystals had to be annealed by blocking the cryostream once for ~2 s to improve diffraction and decrease the mosaicity dramatically. The structure of Pla-Alp11 was solved at 2.0 Å resolution by molecular replacement in Phaser (18) using the high resolution apo-Pla structure (Protein Data Bank (PDB) ID 2X55) as the search model. Model (re)building was performed manually within COOT (19), and the structure was refined using Phenix (20). Structure validation was performed within Phenix. 94.3% of the residues are present in favored regions, 5.3% in allowed regions, and 0.4% in disallowed regions of the Ramachandran plot. Final refinement statistics and analysis are presented in Table 1.

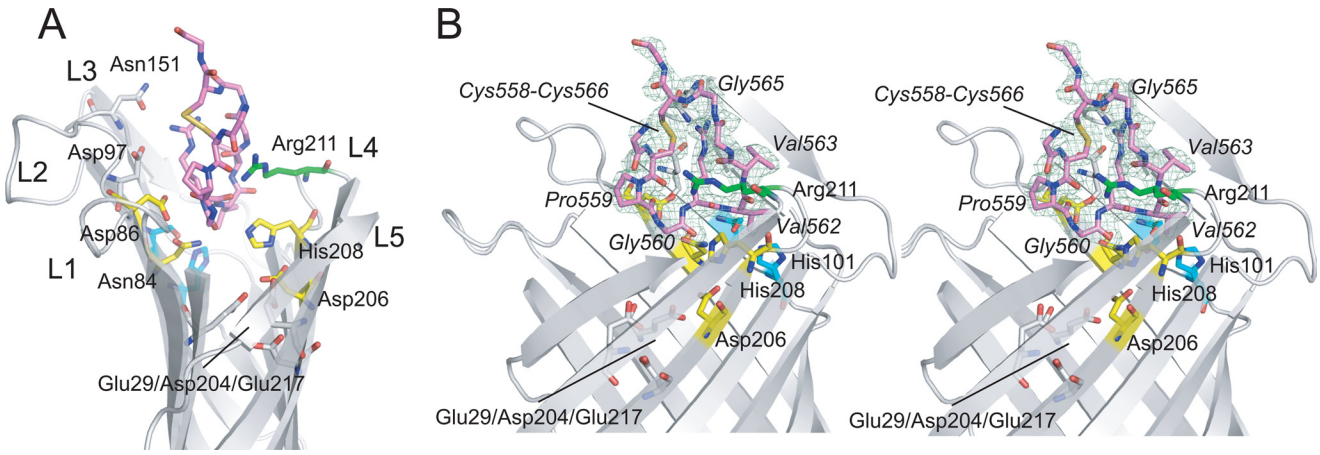

FIGURE 2. **Overview of the Pla-Alp11 structure.** *A*, side view of the extracellular part of the complex shown schematically. Extracellular loops are labeled (*L1–L5*). Alp11 residues (Lys^{557}-Lys^{567}) are shown as *pink stick models*. The Cys^{558}-Cys^{566} disulfide bond is colored *yellow*. The active site residues (Asn^{84}, Asp^{86}, Asp^{206}, and His^{208}) are shown in *yellow*; the other residues that are important for activity are shown in *cyan* (Ser^{99} and His^{101}) and *green* (Arg^{211}). Residues in the two acidic pockets are shown in *gray* (Asp^{97}, Asn^{151}, Glu^{29}, Asp^{204}, and Glu^{217}). *B*, stereoview of the Pla-Alp11 active site from the side, 90° rotated relative to *A*. Residues of the peptide are labeled in *italics*. 2 $F_o - F_c$ map density is shown as a *green mesh*, contoured at 0.7 σ.

Cleavage of Alp11 by Pla D84N—Pla-mediated proteolysis of Alp11 was carried out overnight by incubating Pla D84N purified in β-octylglucoside and Alp11 in the crystallization buffer (45% 2-methyl-2,4-pentanediol, 0.2 M $NH_4KH_2PO_4$, and 0.1 M NaOAc, pH 5.5) at 25 °C. The reaction products were analyzed using electrospray ionization MS (Proteomics and Mass Spectrometry Facility, University of Massachusetts Medical School, Shrewsbury, MA) under nonreducing and reducing (10 mM DTT, 30 min, 60 °C) conditions. The sequences of the resulting peptides were confirmed by tandem mass spectrometry.

RESULTS

Structure of the Pla-Alp11 Complex—Wild-type Pla crystallized only in its LPS-bound active form, even when the protein was extracted and purified in LDAO (11). Moreover, soaking and co-crystallization attempts of peptides with wild-type Pla proved unsuccessful, presumably due to cleavage of the peptide substrate. We therefore employed the low activity (~15% relative to WT) Pla mutant D84N to obtain a 2.0 Å co-crystal structure of Pla in complex with the Alp11 of human plasminogen (Table 1). As is the case for the apo-protein, Pla within the complex forms an ~70 Å long monomeric vase-like barrel that consists of 10 antiparallel β-strands (S1–S10) connected by 5 long extracellular loops (L1–L5). The active site is located in a deep groove formed by the extracellular loops (Fig. 2*A*) and consists of two residue couples: Asn^{84}/Asp^{86} in S3 on one side of the barrel and Asp^{206}/His^{208} in S7 on the other side. The Alp11 peptide is bound within the active site groove, between both active site couples (Fig. 2*A*). In the following discussion, we will use P1 and P1′ for the peptide residues immediately prior to and following the scissile bond, *i.e.* Arg^{561} is the P1 residue and Val^{562} is the P1′ residue (21). The Alp11 peptide is present in the native, oxidized form, with clear density visible for the Cys^{558}-Cys^{566} disulfide bond (Fig. 2*B*) and for most of the peptide. The termini of the peptide are disordered, with Lys^{557} and Lys^{567} modeled as glycine residues due to the absence of side chain density. The density for the scissile peptide bond is clearly continuous, indicating that the peptide substrate has not been cleaved. Given the fact that the D84N Pla mutant has (low) catalytic activity, this result can be explained by the absence of bound LPS in the protein preparation, rendering the enzyme inactive (10). The lack of LPS is due to the fact that the protein was initially purified in LDAO (see "Experimental Procedures"), which removes LPS from its binding site on the outside of the barrel (11). Indeed, the crystal packing of the complex is such that the residues on the outside of the barrel that are normally involved in LPS binding now mediate crystal contacts, making LPS binding physically impossible within the Pla-Alp11 crystal.

LPS-mediated Conformational Changes—What is the effect of LPS removal on the Pla structure? The previously determined structures of apo-Pla in the presence and absence of LPS are very similar, especially in the membrane-embedded regions, with an overall root mean square deviation of 0.42 Å for the C-α atoms (Fig. 3*A*). The biggest structural differences between LPS-free and LPS-containing Pla are found in loops L4 and L5, both of which are present on the side of the barrel where LPS binds (Fig. 3). Most of loop L5 is not visible in the Pla-LPS structure, most likely due to autocatalytic activity at residue Lys^{262} prior to extraction with LDAO (14). Potentially more relevant is the conformation of loop L4 containing the catalytic residues Asp^{206} and His^{208}, as well as the important residue Arg^{211} (13). In the LPS-free structure, the tip of this loop is shifted (~1 Å) outward relative to the structure that contains LPS (Fig. 3*A*). Although this conformational shift would potentially widen the active site groove, the positions of the catalytic residues at the bottom of the groove are essentially unchanged in both structures (differences <0.5 Å). Thus, the structures of apo-Pla in the absence or presence of LPS do not give unambiguous clues as to why LPS removal inactivates the enzyme.

Pla contains an active site water network, linking the catalytic residues and other residues important for enzymatic activity (Fig. 1). One of those water molecules is the putative nucleophilic water, located between Asp^{84} and His^{208} (11). Strikingly, in the Pla-Alp11 structure the peptide has displaced most of the active site waters, including the nucleophilic one (Fig. 3*B*). In

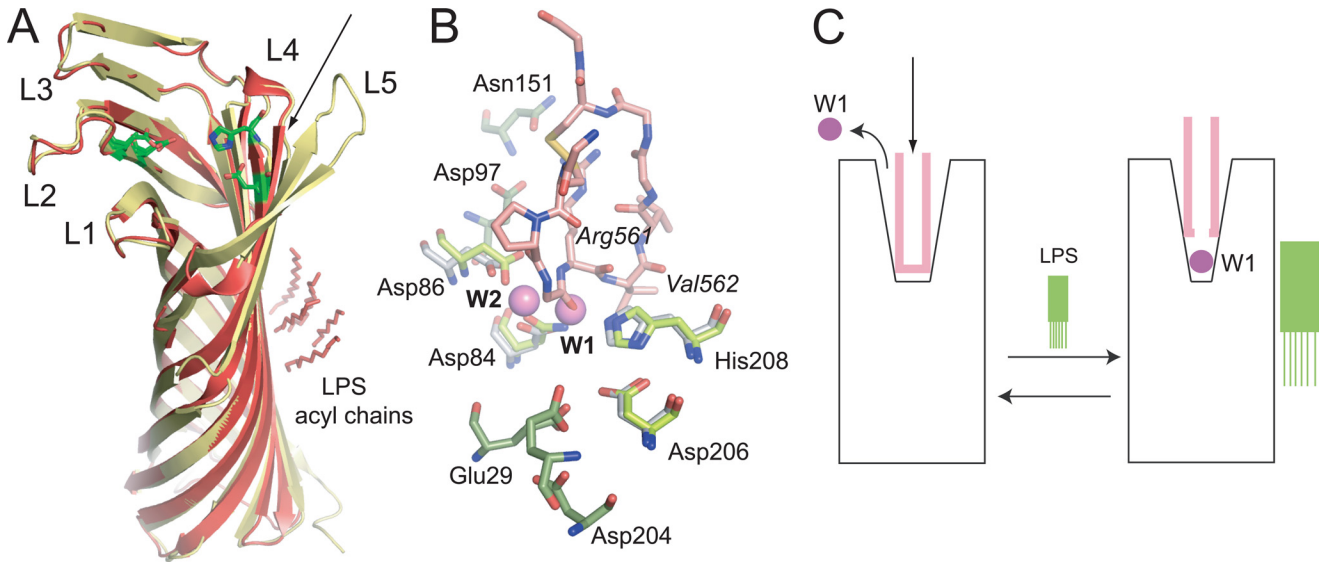

FIGURE 3. **Structure-based model for Pla activation by LPS.** *A*, structural comparison of LPS-free apo-Pla (*yellow*; PDB ID 2X4M) and LPS-bound apo-Pla (*red*; PDB ID 2X55). The active site residues Asp^{84}, Asp^{86}, Asp^{206}, and His^{208} are shown as *green stick models* for both structures. The conformational changes in the tip of loop L4 that arise from LPS binding are indicated with an *arrow*. *B*, close-up of the active site groove of LPS-bound apo-Pla and of the Pla-Alp11 complex. The peptide is colored *salmon*, with oxygens *red* and nitrogens *blue*. The active site residues are shown as *sticks* in *gray* (apo-Pla) and in *green* (Pla-Alp11). The nucleophilic water molecule (*W1*) and the water molecule *W2* between Asp^{84} and Asp^{86} that are present in apo-Pla but absent in Pla-Alp11 are shown as *purple spheres*. Residues within the two acidic binding pockets are shown in *green* for Pla-Alp11 only. *C*, schematic model for Pla activation by LPS. In the absence of LPS (*left*), the activation loop of the substrate (*pink*) binds deep into the active site groove, displacing the nucleophilic water molecule and rendering the enzyme inactive. Upon binding of LPS, the active site groove narrows (*right*). When substrate binds, the catalytic water molecule remains in place to cleave the substrate.

fact, the position of the nucleophilic water molecule in the apo-structure is very close to the carbonyl oxygen atom of the P2 residue Gly^{560} within Pla-Alp11 (Fig. 3*B*). Within the complex, no potential other nucleophile is located close enough to the scissile Arg^{561}-Val^{562} peptide bond to mediate catalysis. We propose that in the absence of LPS, Pla undergoes subtle conformational changes that widen the active site groove. As a result, peptide substrates can diffuse further down into the active site, replacing essential active site water molecules and rendering the enzyme inactive (Fig. 3*C*).

In the Pla-Alp11 complex, the Gly^{560}-Arg^{561} (P2-P1) peptide bond is located between the catalytic residues Asn^{84} and His^{208}, closest to the position where the nucleophilic water would be in the active enzyme. This contrasts with molecular dynamics simulations of *E. coli* OmpT with a short substrate peptide, which placed the scissile (P1-P1′) Arg-Arg peptide bond between the catalytic residues Asp^{83} and His^{208} (OmpT numbering) (12). Extrapolating to Pla, this would mean that the Arg^{561}-Val^{562} peptide bond should be located between Asn^{84} and His^{208}. Moreover, the negatively charged pocket formed by Glu^{29}/Asp^{204}/Glu^{217} and which was proposed to bind the P1 arginine guanidinium group (10, 13), is empty in the structure of the complex (Fig. 3*B*). Instead, the P1 arginine side chain is located at the position of the P1′ side chain in the molecular dynamics simulations, close to Asp^{97} and Asn^{151}. In other words, there is a register shift of one residue between the predictions of the molecular dynamics simulations and our structural data. It is not clear whether the register shift is a consequence of the lack of LPS or whether this is the actual substrate binding mode within the active enzyme. In this context it should be noted that Pla is a very poor enzyme for plasminogen activation, with a k_{cat} of 0.21 min^{-1} (K_m ~120 nM) (22), suggesting that the active site may have an unusual geometry.

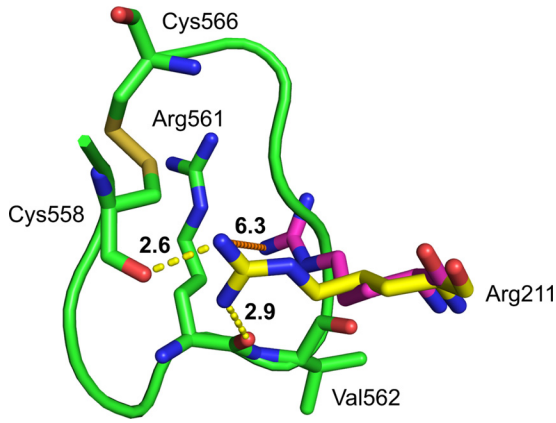

FIGURE 4. **Substrate-induced conformational change of Arg^{211}.** Positions of Arg^{211} in apo-Pla (*magenta*; PDB ID 2X55) and in Pla-Alp11 (*yellow*) are shown in aligned structures. The distance between the arginine side chains in both structures is shown as an *orange dashed line*. Hydrogen bonding between Pla-Alp11 Arg^{211} and the scissile carbonyl as well as the Cys^{558} carbonyl are shown as *yellow dashes*. For simplicity only Arg^{561}, Val^{562}, Cys^{558}, and Cys^{566} in Alp11 are shown as *green stick models*. *Numbers* in *bold* show distances in Å.

Structural studies of active enzyme-substrate complexes as well as biochemical studies based on the current structure will be required to shed light on this issue.

Possible Implications for the Role of Arg^{211}—In the Pla-Alp11 structure the guanidinium group of Arg^{211} moves by 5–6 Å to interact with the peptide substrate (Fig. 4). The arginine side chain forms strong hydrogen bonds with the carbonyl oxygen of Cys^{558}. In addition, a strong hydrogen bond (2.9 Å) is formed with the oxygen atom of the scissile carbonyl group (Fig. 4). Although care must be taken in the interpretation of these structural details because Pla is inactive, the observed interactions might explain the importance of Arg^{211} for catalytic activity. Mutations of this residue to alanine or lysine drastically

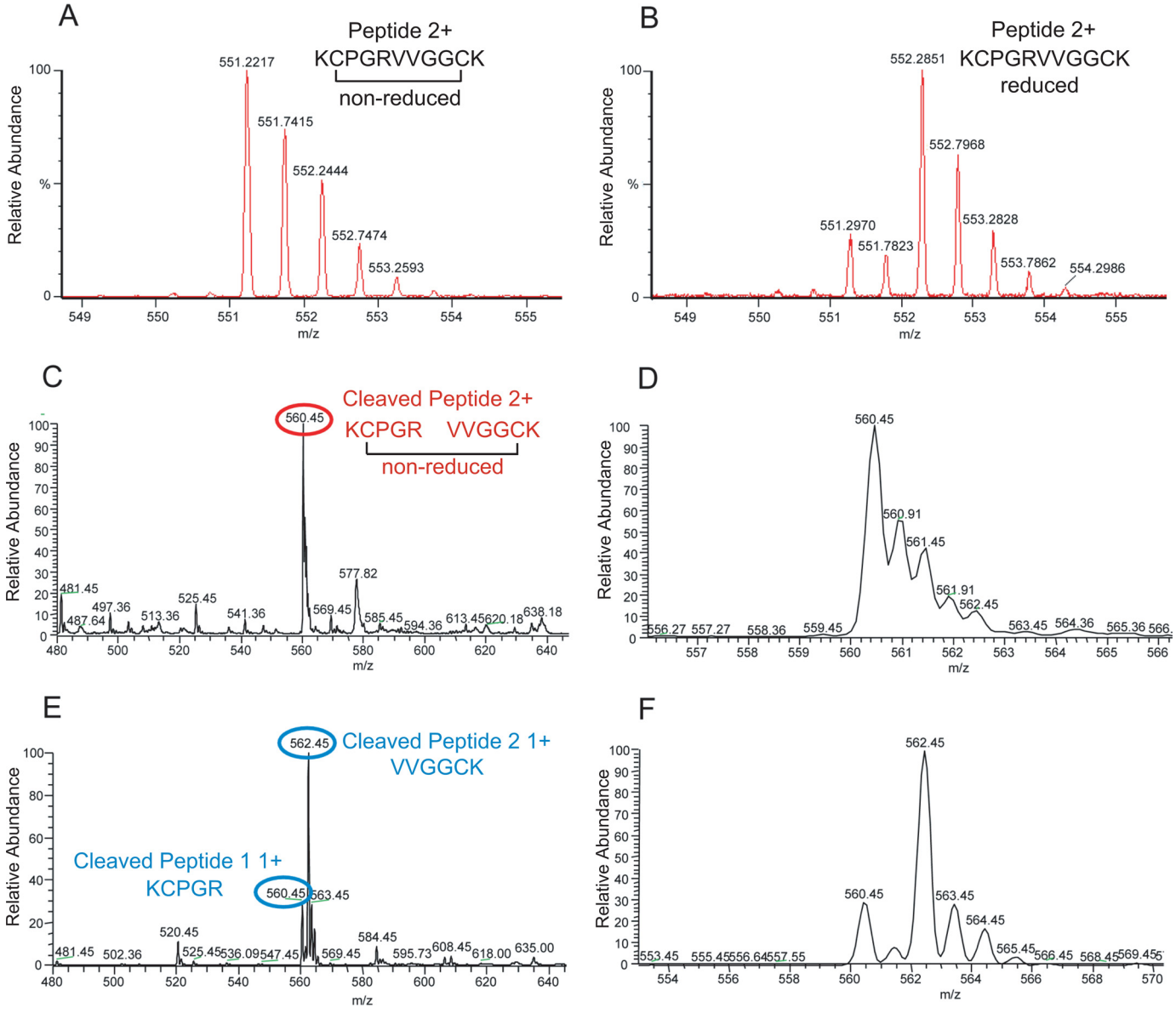

FIGURE 5. **Analysis of Pla-mediated proteolysis of Alp11.** *A*, mass spectrum obtained by infusion of 100 μg of intact Alp11 (expected M2H+ 551.29). *B*, mass spectrum obtained by infusion of 100 μg of reduced Alp11 (expected M2H+ 552.29). *C*, mass spectrum obtained by infusion of 100 ng/μl nonreduced Pla-treated Alp11. Cleaved, disulfide-linked peptide peak (+2) at 560.45 *m/z* is labeled with a *red circle*. (expected M2H+ 560.29). *D*, close-up view of the +2 peak in *C*. *E*, mass spectrum obtained by infusion of 100 ng/μl reduced Pla-treated Alp11. Cleaved peptide 1 (KCPGR; +1) and peptide 2 (VVGGCK; +1) peaks at 560.45 and 562.45 *m/z* are labeled with *blue circles* (peptide 1 (KCPGR) MH+ 559.29; peptide 2 (VVGGCK) MH+ 561.29). *F*, close-up view of the peaks in *E*. The sequences of the resulting peptides were confirmed by tandem mass spectrometry. The values in *parentheses* for *A–F* are the expected (calculated) *m/z* values for the peptides.

lower Pla-mediated cleavage of plasminogen (~1% compared with WT) (11, 13). The observed conformational change of Arg^{211} in the Pla-Alp11 structure may support our previous hypothesis that the positive charge on the arginine side chain could play a role in the stabilization of the oxyanion intermediate during catalysis, in a similar manner to the calcium ion in phospholipase A_2 (23).

Alp11 Proteolysis by Active Pla D84N—To rule out the possibility that the observed position of the Alp11 peptide within the complex is an artifact due to the small size of the peptide relative to full-length plasminogen (~90 kDa), we purified the Pla D84N mutant in β-octylglucoside, ensuring that LPS remains bound on the outside of the barrel and preserving enzymatic activity (11). After incubating the protease with the Alp11 peptide in crystallization buffer (see "Experimental Procedures"), the reaction products were analyzed by mass spectrometry (Fig. 5). The results show that (i) the Alp11 peptide is present in the oxidized form, (ii) Pla D84N is active and cleaves Alp11 in the crystallization buffer, and (iii) the Arg^{561}-Val^{562} peptide bond is cleaved, identical to the cleavage site in full-length human plasminogen (22). We conclude that the Alp11 peptide is a genuine substrate of Pla that is cleaved in the same way as its physiological macromolecular substrate, provided that LPS is bound to the protein.

DISCUSSION

The structural data presented here provide an explanation for the LPS dependence of omptins for enzymatic activity. An

interesting question is why omptins require LPS to be active. By virtue of the fact that the outer leaflet of the OM consists almost exclusively of LPS, omptin activity will always be turned on. Together with the fact that a number of different forms of LPS can activate omptins (15), it is therefore unlikely that LPS serves as a regulator of Pla activity within the OM. An alternative, intriguing possibility is that the requirement for LPS is a consequence of a need to keep the protease inactive within the periplasmic space during OM targeting and integration. This hypothesis would extend the known roles of lipid allostery in membrane protein function and would imply that native-like structure in OM proteins could be formed prior to their insertion into the OM.

Acknowledgments—We thank the staff of NSLS beamline X6A for beam time and for assistance during data collection and Stephanie Maniatis for mass spectrometry analysis.

REFERENCES

1. Coskun, U., and Simons, K. (2011) Cell membranes: the lipid perspective. *Structure* **19,** 1543–1548
2. Hansen, S. B., Tao, X., and MacKinnon, R. (2011) Structural basis of PIP_2 activation of the classical inward rectifier K^+ channel Kir2.2. *Nature* **477,** 495–498
3. Oates, J., and Watts, A. (2011) Uncovering the intimate relationship between lipids, cholesterol, and GPCR activation. *Curr. Opin. Struct. Biol.* **21,** 802–807
4. Plow, E. F., Ploplis, V. A., Busuttil, S., Carmeliet, P., and Collen, D. (1999) A role of plasminogen in atherosclerosis and restenosis models in mice. *Thromb. Haemost.* **82,** 4–7
5. Sebbane, F., Jarrett, C. O., Gardner, D., Long, D., and Hinnebusch, B. J. (2006) Role of the *Yersinia pestis* plasminogen activator in the incidence of distinct septicemic and bubonic forms of flea-borne plague. *Proc. Natl. Acad. Sci. U.S.A.* **103,** 5526–5530
6. Lathem, W. W., Price, P. A., Miller, V. L., and Goldman, W. E. (2007) A plasminogen-activating protease specifically controls the development of primary pneumonic plague. *Science* **315,** 509–513
7. Haiko, J., Suomalainen, M., Ojala, T., Lähteenmäki, K., and Korhonen, T. K. (2009) Invited review. Breaking barriers: attack on innate immune defences by omptin surface proteases of enterobacterial pathogen. *Innate Immun.* **15,** 67–80
8. Hritonenko, V., and Stathopoulos, C. (2007) Omptin proteins: an expanding family of outer membrane proteases in Gram-negative Enterobacteriaceae. *Mol. Membr. Biol.* **24,** 395–406
9. Kukkonen, M., and Korhonen, T. K. (2004) The omptin family of enterobacterial surface proteases/adhesins: from housekeeping in *Escherichia coli* to systemic spread of *Yersinia pestis*. *Int. J. Med. Microbiol.* **294,** 7–14
10. Vandeputte-Rutten, L., Kramer, R. A., Kroon, J., Dekker, N., Egmond, M. R., and Gros, P. (2001) Crystal structure of the outer membrane protease OmpT from *Escherichia coli* suggests a novel catalytic site. *EMBO J.* **20,** 5033–5039
11. Eren, E., Murphy, M., Goguen, J., and van den Berg, B. (2010) An active site water network in the plasminogen activator Pla from *Yersinia pestis*. *Structure* **18,** 809–818
12. Baaden, M., and Sansom, M. S. (2004) OmpT: molecular dynamics simulations of an outer membrane enzyme. *Biophys J.* **87,** 2942–2953
13. Kramer, R. A., Vandeputte-Rutten, L., de Roon, G. J., Gros, P., Dekker, N., and Egmond, M. R. (2001) Identification of essential acidic residues of outer membrane protease OmpT supports a novel active site. *FEBS Lett.* **505,** 426–430
14. Kukkonen, M., Lähteenmäki, K., Suomalainen, M., Kalkkinen, N., Emödy, L., Lång, H., and Korhonen, T. K. (2001) Protein regions important for plasminogen activation and inactivation of α_2-antiplasmin in the surface protease Pla of *Yersinia pestis*. *Mol. Microbiol.* **40,** 1097–1111
15. Kramer, R. A., Brandenburg, K., Vandeputte-Rutten, L., Werkhoven, M., Gros, P., Dekker, N., and Egmond, M. R. (2002) Lipopolysaccharide regions involved in the activation of *Escherichia coli* outer membrane protease OmpT. *Eur. J. Biochem.* **269,** 1746–1752
16. Kukkonen, M., Suomalainen, M., Kyllönen, P., Lähteenmäki, K., Lång, H., Virkola, R., Helander, I. M., Holst, O., and Korhonen, T. K. (2004) Lack of *O*-antigen is essential for plasminogen activation by *Yersinia pestis* and *Salmonella enterica*. *Mol. Microbiol.* **51,** 215–225
17. Otwinowski, Z., and Minor, W. (1997) Processing of x-ray diffraction data collected in oscillation mode. *Methods Enzymol.* **276,** 307–326
18. Storoni, L. C., McCoy, A. J., and Read, R. J. (2004) Likelihood-enhanced fast rotation functions. *Acta Crystallogr. D Biol. Crystallogr.* **60,** 432–438
19. Emsley, P., and Cowtan, K. (2004) COOT: model-building tools for molecular graphics. *Acta Crystallogr. D Biol. Crystallogr.* **60,** 2126–2132
20. Adams, P. D., Grosse-Kunstleve, R. W., Hung, L. W., Ioerger, T. R., McCoy, A. J., Moriarty, N. W., Read, R. J., Sacchettini, J. C., Sauter, N. K., and Terwilliger, T. C. (2002) PHENIX: building new software for automated crystallographic structure determination. *Acta Crystallogr. D Biol. Crystallogr.* **58,** 1948–1954
21. Schechter, I., and Berger, A. (1967) On the size of the active site in proteases. I. Papain. *Biochem. Biophys. Res. Commun.* **27,** 157–162
22. Sodeinde, O. A., Subrahmanyam, Y. V., Stark, K., Quan, T., Bao, Y., and Goguen, J. D. (1992) A surface protease and the invasive character of plague. *Science* **258,** 1004–1007
23. Scott, D. L., White, S. P., Otwinowski, Z., Yuan, W., Gelb, M. H., and Sigler, P. B. (1990) Interfacial catalysis: the mechanism of phospholipase A_2. *Science* **250,** 1541–1546